The Journal of Immunology

Neonatal Follicular Th Cell Responses Are Impaired and Modulated by IL-4

Isabelle Debock, Kathy Jaworski, Hanan Chadlaoui, Sandrine Delbauve, Nicolas Passon, Laure Twyffels, Oberdan Leo and Véronique Flamand

J Immunol 2013; 191:1231-1239; Prepublished online 26 June 2013;
doi: 10.4049/jimmunol.1203288
http://www.jimmunol.org/content/191/3/1231

The Journal of Immunology is published twice each month by
The American Association of Immunologists, Inc.,
9650 Rockville Pike, Bethesda, MD 20814-3994.

Print ISSN: 0022-1767 Online ISSN: 1550-6606.

Neonatal Follicular Th Cell Responses Are Impaired and Modulated by IL-4

Isabelle Debock,*,[1] Kathy Jaworski,*,[1] Hanan Chadlaoui,* Sandrine Delbauve,* Nicolas Passon,* Laure Twyffels,†,‡ Oberdan Leo,* and Véronique Flamand*

Newborns are characterized by poor responses to vaccines. Defective B cell responses and a Th2-type polarization can account for this impaired protection in early life. We in this study investigated the generation of follicular Th (T_{FH}) cells, involved in the development of Ab response and germinal center reaction, upon vaccination in neonates. We showed that, compared with adults, Ab production, affinity maturation, and germinal center formation were reduced in neonates immunized with OVA–aluminum hydroxide. Although this vaccination induced $CD4^+$ $CXCR5^+$ $PD\text{-}1^+$ T_{FH} cells in newborns, their frequency, as well as their Bcl6 expression and IL-21 and IL-4 mRNA induction, was decreased in early life. Moreover, neonatal T_{FH} cells were mainly localized in interfollicular regions of lymphoid tissues. The prototypic Th2 cytokine IL-4 was found to promote the emergence and the localization in germinal centers of neonatal T_{FH} cells, as well as the neonatal germinal center reaction itself. In addition, IL-4 dampened expression of Th17-related molecules in neonatal T_{FH} cells, as T_{FH} cells from immunized IL-4–deficient neonates displayed enhanced expression of RORγt and IL-17. This Th17-like profile correlated with an increased secretion of OVA-specific IgG2a. Our study thus suggests that defective humoral immunity in early life is associated with limited and IL-4–modulated T_{FH} cell responses. *The Journal of Immunology*, **2013, 191: 1231–1239.**

Neonates and young children typically present poor responses to vaccines (1). This weak responsiveness is associated with low protection and heightened sensitivity to pathogens in early life (2). Indeed, Ab production and B cell immune responses are defective in newborns (3). Different factors of the neonatal immune system can account for these impairments. The microarchitecture of secondary lymphoid organs that is needed to support optimal Ab responses is developing during the first weeks of life (4). Furthermore, neonatal progenitors of follicular dendritic cells (FDC) are unresponsive to differentiation signals provided by neonatal B cells, leading to a delayed induction and maturation of a functional FDC network (5). At the level of B lymphocytes, the differentiation pathway to memory B cells is favored in early life, at the expense of Ab-producing plasma cells (3). In addition, homing to and colonization of the bone marrow by plasma cells are limited in newborns (3, 6). A bias toward the Th2 subset is also at play in neonates, whereas IFN-γ–producing Th1 responses are deficient (7). This Th2 immune deviation is associated with Th cell–intrinsic epigenetic modifications allowing an enhanced secretion of the canonical Th2 cytokine IL-4 (8). Moreover, IL-4 reinforces the neonatal Th2 bias by driving apoptosis of primary Th1 cells (9) and by inhibiting the development of Th17 cells (10).

$CD4^+$ T cell help is essential for full B cell responses, including germinal center (GC) reaction, isotype class switching, and Ab affinity maturation. These features were first attributed to Th2 cells, IL-4 being involved in B cell stimulation and class switch recombination to IgG1 and IgE (11–13). Recently, follicular Th (T_{FH}) cells were described as the specialized providers of B cell help. T_{FH} cells produce IL-21 and express high levels of the CXCL13 chemokine receptor CXCR5, allowing them to relocate in B cell follicles, as well as the costimulatory ICOS and inhibitory PD-1 molecules (14). The transcriptional repressor Bcl6 was identified as the master regulator of the T_{FH} pathway, establishing T_{FH} cells as a distinct helper T cell subset (15–17). Bcl6 indeed inhibits the expression or function of T-bet, GATA3, and RORγt, master regulators of the Th1, Th2, and Th17 lineages, respectively (16). Whereas T_{FH} cell differentiation is still a matter of debate, it requires the presence of dendritic cells and B cells as APCs (18), as well as ICOS signaling that induces the expression of Bcl6 and subsequently of CXCR5 (19). IL-6 and IL-21, both cytokines activating the transcription factor STAT3, are also contributive to the emergence of T_{FH} cells (20–22).

Given that B cell and vaccine responses are impaired in early life, we sought to investigate the generation and function of T_{FH} cells in mouse newborns by both in vitro and in vivo models.

Materials and Methods

Mice

BALB/c ($H\text{-}2^d$) were purchased from Harlan, and IL-4 knockout mice from The Jackson Laboratory (Bar Harbor, ME). Mice were bred and housed in our specific pathogen-free facility. All animal studies were approved by the institutional animal care and local use committee.

*Institut d'Immunologie Médicale, Université Libre de Bruxelles, 6041 Gosselies, Belgium; †Laboratoire de Biologie Moléculaire du Gène, Université Libre de Bruxelles, 6041 Gosselies, Belgium; and ‡Centre de Microscopie et d'Imagerie Moléculaire, 6041 Gosselies, Belgium

[1]I.D. and K.J. contributed equally to this work.

Received for publication November 29, 2012. Accepted for publication May 23, 2013.

The Institute for Medical Immunology is supported by the government of the Walloon Region and GlaxoSmithKline Biologicals. This work was also supported by Fonds National de la Recherche Scientifique (Belgium) and the Interuniversity Attraction Pole of the Belgian Federal Science Policy. I.D. is supported by a grant from Fondation Rose et Jean Hoguet, and K.J. is supported by a grant from Fonds Européen de Développement Régional-CONVERGENCE.

Address correspondence and reprint requests to Dr. Véronique Flamand, Institute for Medical Immunology, Université Libre de Bruxelles, Rue Adrienne Bolland 8, 6041 Gosselies, Belgium. E-mail address: vflamand@ulb.ac.be

The online version of this article contains supplemental material.

Abbreviations used in this article: Alum, aluminum hydroxide; FDC, follicular dendritic cell; GC, germinal center; IFR, interfollicular region; mLN, mesenteric lymph node; NP, nuclear protein; PNA, peanut agglutinin; T_{FH}, follicular Th; WT, wild-type.

www.jimmunol.org/cgi/doi/10.4049/jimmunol.1203288

In vivo treatments

Eight- to 10-wk-old adult and neonatal 7-d-old mice were immunized by i.p. injection of 50 μg OVA (Worthington Biochemical) or 100 μg nuclear protein (NP)–keyhole limpet hemocyanin (Biosearch Technologies) in 100 μl aluminum hydroxide (Alum; Reheis Chemical) and 12.5 μg OVA or 25 μg NP–keyhole limpet hemocyanin in 25 μl Alum, respectively. A boost was performed 3 wk after the primary immunization. Blood serum was collected at the indicated intervals.

In vitro cell culture

Cell cultures were performed in RPMI 1640 medium (Lonza Research Products) supplemented with 20 mM HEPES, 2 mM L-glutamine, 1 mM nonessential amino acids (Lonza Research Products), 5% heat-inactivated FCS, 100 mM sodium pyruvate (Lonza Research Products), penicillin (10 U/ml)-streptomycin (10 μg/ml), and 10^{-5} M 2-ME. Cultures were kept at 37°C in 5% CO_2 atmosphere. $CD4^+$ T cells were isolated from spleens of pools of adult ($n = 4$) and neonatal ($n = 20$) mice using the CD4 (L3T4) magnetic MicroBeads (Miltenyi Biotec, Auburn, CA) on an AutoMACS separator (Miltenyi Biotec), according to manufacturer's instructions. B cells were isolated from spleens of pools of adult mice using the Dynabeads Mouse CD43 untouched B cells kit (Dynal, Invitrogen) or the B cell isolation kit (Miltenyi Biotec), according to manufacturer's instructions. Purity of cell suspensions was routinely determined by flow cytometry (>90%). $CD4^+$ T cells (1×10^6 cells/ml/well in 48-well plates) were activated for 48 h with 10 μg/ml plastic-coated anti-CD3 mAbs (clone 145-2C11; BD Biosciences) and 2.5 μg/ml soluble anti-CD28 mAbs (clone 37.51; BD Biosciences), with or without 20 ng/ml rIL-6 (R&D Systems). After 48 h, supernatants were harvested for cytokine detection and T cells were recovered, extensively washed, and rested for 24 h in culture medium. T cells were then irradiated (2000 rad), and serial dilutions of T cells (1×10^5 to 1×10^3 cells/well) were cultured for 7 d in 96-well plates with syngeneic B cells (5×10^5 cells/well) in the presence of 2 μg/ml anti-CD3 mAbs in 200 μl culture medium. Supernatants were harvested 7 d later and tested for Ig secretion.

Cytokine production assays and in vitro Ig levels

Cytokine concentrations in supernatants were assessed by ELISA using commercially available kits (Duoset; R&D Systems). Ig levels were determined by sandwich ELISAs using purified rat IgG1κ or IgG2aκ directed against γ1 (clone LO-MG1-13, Lo-Imex, UCL), ε (clone LO-ME-3), γ2a (clone LO-MG2a-9), and Lκ (clone LO-MK-2) H chains of mouse IgG1, IgE, IgG2a, and total Ig as capture mAb, respectively, and purified biotinylated rat IgG1κ or IgG2aκ directed against γ1 (clone LO-MG1-2, Lo-Imex, UCL), ε (clone LO-ME-2), γ2a (clone LO-MG2a-7), and Lκ (clone LO-MK-1) H chains as detection mAb. Standard curves were generated with purified mouse IgG1 (clone MADNP-1), IgE (clone C38-2; BD Biosciences), IgG2a (clone MADNP-2), and mouse serum IgG (Sigma-Aldrich) for total Ig quantification.

OVA-specific Ig levels

OVA-specific total Ig, IgG1, and IgG2a serum levels were determined by ELISA. For total Ig and IgG1 quantification, OVA-coated (10 μg/ml; Sigma-Aldrich) Maxisorp plates (Nunc, Langenselbold, Germany) were incubated with serial dilutions of sera and biotinylated mAb to total Ig (clone LO-MK-1) or to IgG_1 (clone LO-MG1-2). For IgG2a quantification, plates were first coated with capture mAb to IgG2a (LO-MG2a-9) and then incubated with serial dilutions of sera and biotinylated OVA (Immunosource). OVA-specific Ig titers were expressed as relative values to hyperimmune sera used as reference.

Affinity maturation assay

Affinity of serum NP-specific IgE was determined by ELISA. Maxisorp ELISA plates (Nunc) were coated with NP-BSA conjugates (Biosearch Technologies) at two different hapten concentrations, NP_5 and NP_{16}. NP_{16}-BSA conjugates are bound by high- and low-affinity NP-specific IgE, whereas NP_5-BSA conjugates are only bound by high-affinity IgE. Biotinylated rat anti-Hε mAb (clone LO-ME-2, Lo-Imex, UCL) were used as detection mAb. IgE values were expressed as a NP_5/NP_{16} ratio in arbitrary units compared with values of hyperimmune sera used as reference.

Flow cytometry and cell sorting

For intracellular staining, anti-CD3/CD28–activated $CD4^+$ T cells in the presence or not of IL-6 were incubated with 1 μM monensin (eBioscience) for the last 4 h of the 48-h culture at 37°C. After blocking of FcRs (anti-CD16/CD32 mAbs, clone 39; eBioscience), cells were stained with anti-CD4 Pacific Blue or FITC (clone RM4-5), anti-CXCR5 biotin (clone 2G8) and streptavidin-V450, anti-ICOS biotin (clone 7E.17G9; eBioscience) plus streptavidin-APC, and anti–PD-1 FITC (clone J43; eBioscience). Then cells were fixed and permeabilized with CytoFix/CytoPerm (BD Biosciences) and stained with anti–IL-4 APC (clone 11B11), anti–IL-10 APC (clone JES5-16E3), anti–IL-17A Alexa Fluor (clone TC11-18H10; BD Biosciences), or isotype controls. IL-21 detection was performed with soluble IL-21R subunit/Fc chimeric protein (R&D Systems) and PE-labeled goat anti-human IgG (Jackson ImmunoResearch Laboratories). For ex vivo T_{FH} experiments, mesenteric lymph node (mLN) cells were first incubated at 37°C for 30 min. After washing and blocking of FcRs, cells were stained with anti-CXCR5 biotin (clone 2G8) for 45 min at room temperature, and with streptavidin-PE, anti-CD4 Pacific Blue, anti-CD19 APC-Cy7 (clone 1D3), and anti–PD-1 FITC for 20 min at 4°C or with anti-CXCR5 biotin for 45 min at room temperature, and with streptavidin-V450, anti-CD4 FITC, anti-CD19 APC-Cy7, and anti-CCR7 PE (clone 4B12) or anti–PSGL-1 PE (clone 2PH1) for 20 min at 4°C. When indicated, cells were then fixed and permeabilized using the Foxp3 Staining Buffer Set (eBioscience) and stained with anti-Bcl6 Alexa Fluor 647 (clone K112-91) or isotype control for 45 min at 4°C. Cells were analyzed on a Cyan ADP flow cytometer (DakoCytomation, Glostrup, Denmark). Doublets and dead cells were always excluded based on the forward/side light scatter profiles. For T_{FH} cell sorting, mLN cells were stained following the same protocol as above, with the exception that anti-CD3 APC (clone 500A2) mAb were used instead of anti-CD19 APC-Cy7 mAb. $CD4^+$ $CD3^+$ $CXCR5^+$ $PD1^+$ T_{FH} and $CD4^+$ $CD3^+$ $CXCR5^-$ $PD1^-$ non-T_{FH} cells were sorted out using a Moflo cell sorter (DakoCytomation). Cells were then lysed in TRIzol (TriPure Isolation Reagent; Roche Diagnostics) for RNA extraction and quantitative real-time PCR. All Abs, excepted where otherwise indicated, were purchased from BD Biosciences.

Quantification of transcripts

Total RNA from FACS-sorted cells was extracted with phenol/chloroform and purified with the RNeasy microkit (Qiagen), according to manufacturer's instructions. Reverse transcription and quantitative real-time PCR were performed in a single step using the TaqMan RNA Amplification (Roche Diagnostics) on a Lightcycler 480 apparatus (Roche Diagnostics). For individual samples, mRNA levels were normalized to those of β-actin used as reference. The sequence of primers and probes is available on request.

Histology and confocal microscopy

mLN sections were stained with H&E, after fixation in 10% formalin neutral solution and paraffin embedding. GC analysis was performed by immunostaining using biotinylated rat anti-mouse CD45R/B220 (BD Biosciences) or biotinylated peanut agglutinin (PNA; Vector Laboratories) plus streptavidin-HRP and diaminobenzidine substrate (DAB Substrate Kit; BD Biosciences). $B220^+$ PNA^+ GC B cells were counted on an average of 15–20 follicles per slide. For immunofluorescence, paraffin-embedded sections from mLNs were incubated with rabbit polyclonal anti-CD3 (Abcam), biotinylated anti-CD45R/B220, and anti-Bcl6 Alexa Fluor 647 (BD Biosciences) after Ag retrieval with Tris-EDTA buffer. Sections were then stained with goat anti-rabbit IgG Alexa Fluor 546 (Life Technologies) and streptavidin Horizon V450 (BD Biosciences). All images were acquired on a Zeiss LSM 710 confocal microscope equipped with a ×20/0.8 Plan-Apochromat dry objective. The size of GC per each follicle and quantitative measurements were performed using the Image J software.

Statistics

Data are expressed as mean ± SEM. Statistical comparison between group means was analyzed using a two-tailed nonparametric Mann–Whitney U test. The p values < 0.05 were considered significant.

Results

IL-6–polarized neonatal $CD4^+$ T cells display features of T_{FH} cells in vitro

We evaluated the capacity of neonatal $CD4^+$ T cells to acquire characteristics of T_{FH} cells upon in vitro culture under T_{FH}-polarizing conditions, as previously described (20). We first observed by cytometry that IL-6 could induce similar proportions of IL-21–producing $CD4^+$ T cells in adults and 7-d-old newborns (Fig. 1A). These IL-21–producing $CD4^+$ T cell subsets from both ages displayed features of T_{FH} cells as measured by CXCR5, Bcl6, PD-1, and ICOS expression among them. Adult IL-21 producers dis-

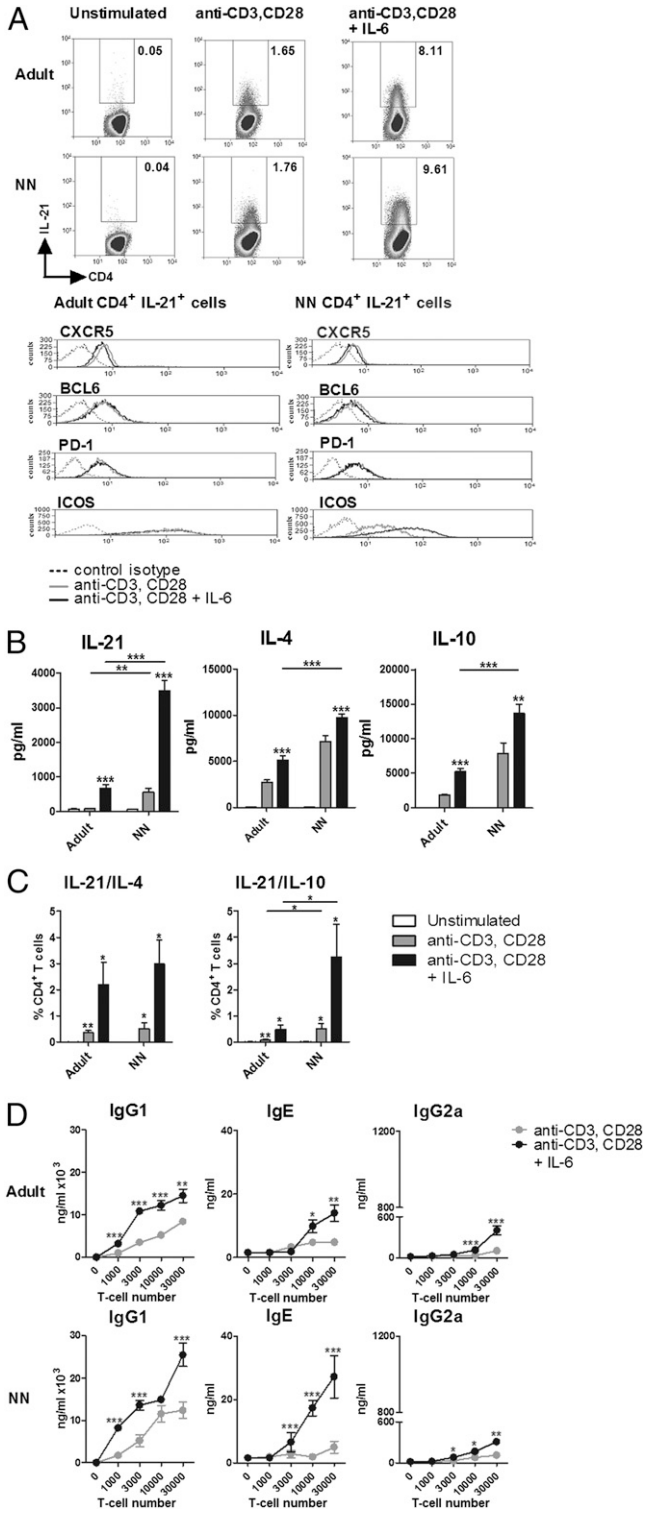

FIGURE 1. IL-6 polarizes neonatal CD4$^+$ T cells to T_{FH} cells. CD4$^+$ T cells isolated from spleens of 8-wk-old (pool of 4) adult and 7-d-old neonatal mice (pool of 20) were stimulated with anti-CD3 and anti-CD28 mAb in the presence or absence of IL-6. (**A**) Representative flow cytometric analysis of three experiments of the percentages of IL-21–producing CD4$^+$ cells and of CXCR5, Bcl6, PD-1, and ICOS expression among them. (**B**) Cytokine levels in supernatants were measured by ELISA. (**C**) Intracellular staining of IL-21 and either IL-4 or IL-10 in T cells. Results are expressed as percentages of cytokine-producing cells among CD4$^+$ T cells. (B and C) Data are mean values ± SEM collected from four independent experiments each performed with triplicate culture of pooled groups of 4 adult and 20 neonatal mice. (**D**) After 24 h of resting, CD4$^+$ T cells were cocultured with B cells isolated from spleens of 8-wk-old adult mice in the presence of anti-CD3 mAb. Ig levels in supernatants were quantified by ELISA. Data are mean values ± SEM from five independent experiments each performed with quadruplicate cultures of pooled groups of 4 adult and 20 neonatal mice. *$p < 0.05$, **$p < 0.005$, ***$p < 0.001$.

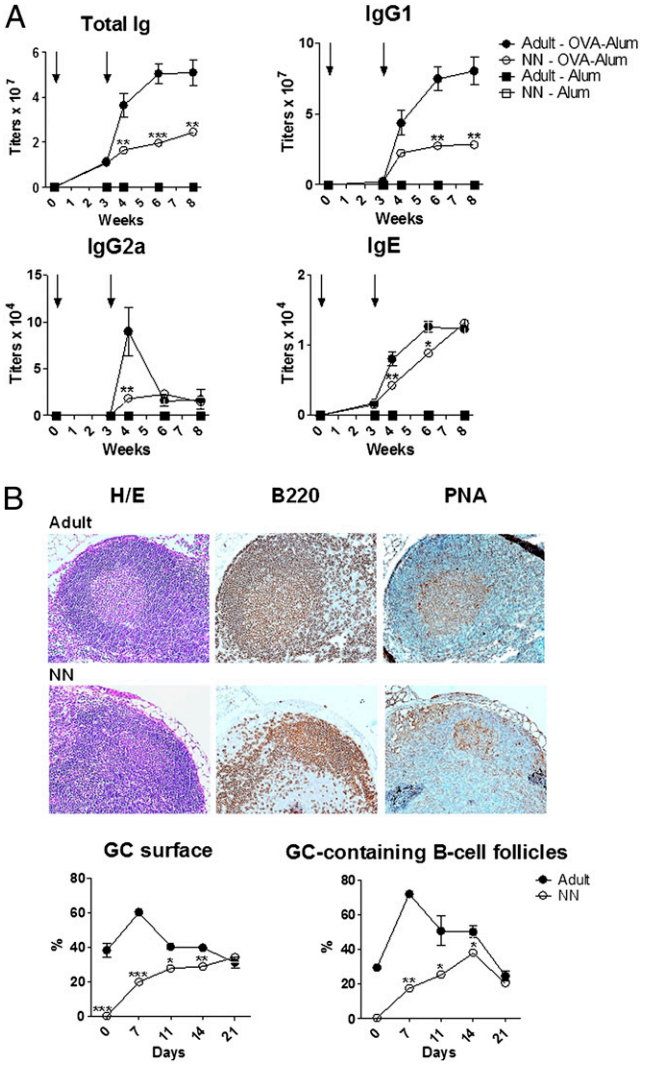

FIGURE 2. Defective humoral response in early life. Eight-wk-old and 7-d-old mice were immunized with OVA and alum. (**A**) OVA-specific serum Ig levels from 8-wk-old ($n = 5$) and 7-d-old ($n = 11$) mice were determined by ELISA. As control, Ig levels from 8-wk-old ($n = 5$) and 7-d-old ($n = 6$) mice injected with Alum were determined by ELISA. (**B**) Histology of mLN was carried out to determine the presence of GC in B cell follicles identified by anti-B220 or PNA staining (brown). Representative sections from immunized adults ($n = 5$) and neonates ($n = 5$) were selected 2 wk after immunization (original magnification ×40). Graphs represent the percentage of B cell follicles containing at least one GC and the proportion of GC surface versus the B cell follicle surface. Data were collected from three independent experiments. *$p < 0.05$, **$p < 0.005$, ***$p < 0.001$.

played optimal expression of CXCR5, Bcl6, PD-1, and ICOS, as did neonatal IL-21 producers for CXCR5 and PD-1. Compared with adult cells, neonatal CD4$^+$ T cells presented lower expression of Bcl6 (4.8 ± 0.3 mean fluorescence intensity in neonates versus 8.1 ± 0.2 mean fluorescence intensity in adults), even when stimulated with IL-6, whereas the expression of ICOS on neonatal CD4$^+$ T cells was low under neutral conditions, but reached levels comparable to their adult counterparts upon IL-6 stimulation.

Compared with adults, neonatal T_{FH}-conditioned T cells secreted high levels of IL-21, as well as IL-4 and IL-10 (Fig. 1B). In addition, adult and neonatal IL-21–producing T cells concomitantly produced IL-4 or IL-10, the proportions of these double producers being strongly increased by IL-6 (Fig. 1C). Whereas the percentages of IL-21/IL-4–producing cells were similar between adult and newborn T_{FH}-polarized T cells, we detected higher proportions of IL-21/IL-10–producing cells in neonates. In these settings, single producers of IL-17, as well as IL-17/IL-21 double producers, were negligible at both ages and not significantly affected in these IL-6–supplemented cultures (Supplemental Fig. 1). To investigate the ability of neonatal T cells to provide B cell help, we cocultured neonatal T_{FH}-polarized $CD4^+$ T cells with adult B cells and we assessed Ab secretion (Fig. 1D). IL-6–polarized adult T cells increased the production of IgG1, IgE, and IgG2a in comparison with unpolarized T cells. We observed that, when neonatal T_{FH}-polarized T cells were present in the B cell culture, the amounts of IgG1, IgG2a, and more particularly IgE were in-

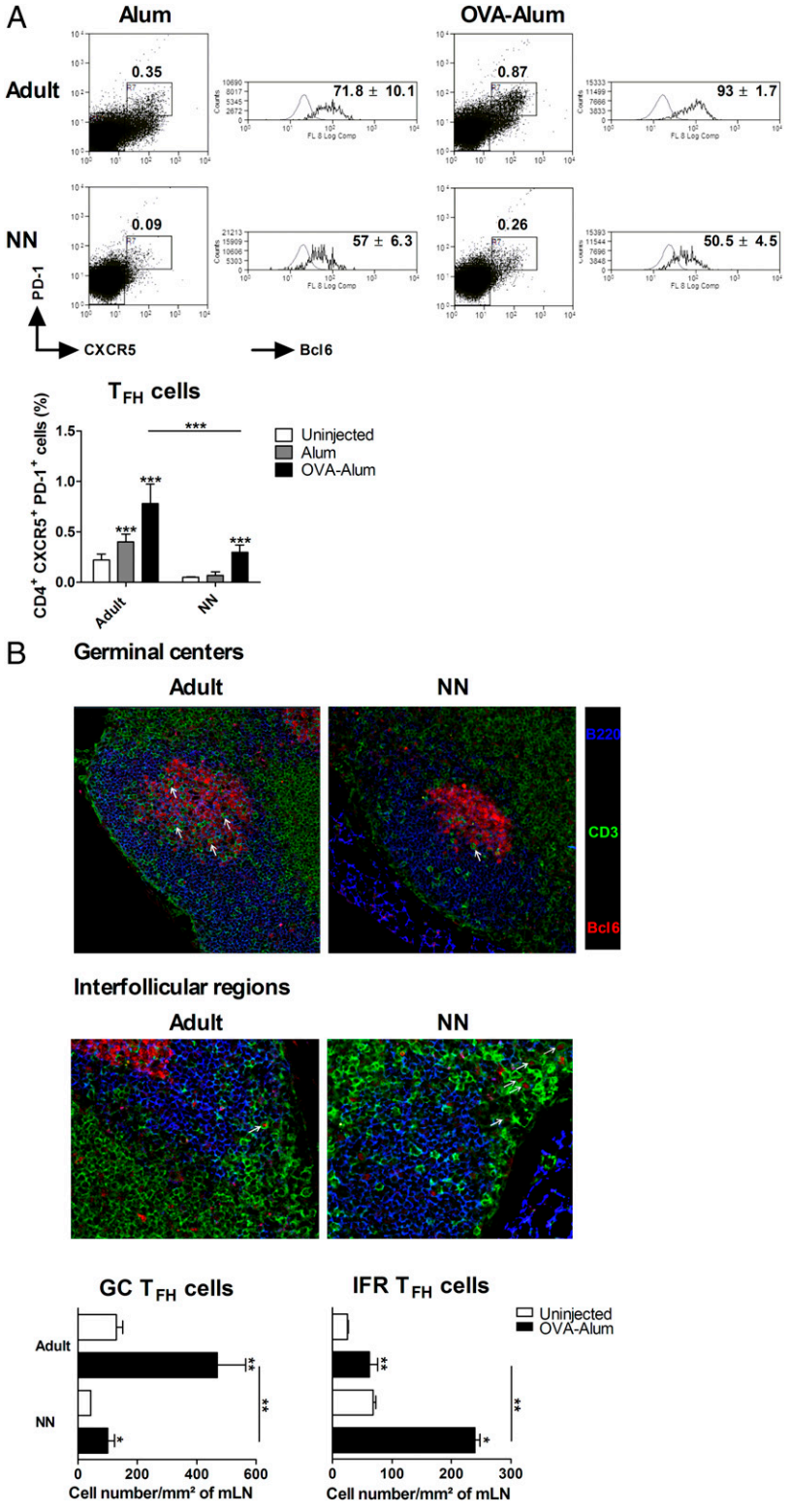

FIGURE 3. Neonatal T_{FH} cells display limited development and localization to GC. (**A**) Representative dot plots of $CD4^+$ $CD19^-$ $CXCR5^+$ $PD\text{-}1^+$ T_{FH} cells in mLN from 8-wk-old adult and 7-d-old neonatal immunized mice on day 7 postimmunization. Histograms show intranuclear expression of Bcl6 in T_{FH} cells (black line) and non-T_{FH} cells (gray line). Values indicated median fluorescence intensities of Bcl6 expression. Plotted values are presented in graph. Groups contained two to seven mice. (**B**) Immunofluorescence staining of mLN sections was performed to localize $CD3^+$ $Bcl6^+$ T_{FH} cells in GC ($B220^+$ $Bcl6^+$ B cells) and in IFR ($CD3^+$ $B220^+$ regions). Representative sections from immunized adults ($n = 5$) and newborns ($n = 5$) were selected on day 7 or 14 postimmunization, respectively (original magnification ×100). Graphs represent absolute numbers of GC T_{FH} cells and IFR T_{FH} cells. Values were normalized to the surface of mLN. Data were collected from two independent experiments. $*p < 0.05$, $**p < 0.005$, $***p < 0.001$.

creased, indicating that neonatal T cells can promote Ab secretion and isotype class switching. Altogether, these results suggest that neonatal T cells can develop features of T_{FH} cells in vitro.

Neonatal immunization induces limited Ab production and GC reaction

To investigate the development of a T_{FH} cell response and its consequences in vivo, we immunized adult and newborn mice with OVA and Alum and first analyzed Ab production and affinity. Compared with adult serum titers, immunized newborns presented a decreased secretion of total OVA-specific Ig (Fig. 2A). We observed a similar reduction in the levels of OVA-specific IgG1 and IgG2a, whereas neonatal IgE titers were less affected. Evaluation of affinity maturation revealed that neonatal IgE displayed lower affinity compared with adult IgE (Supplemental Fig. 2). Because affinity maturation occurs preferentially in GC, we assessed the status of GC in neonates using H&E, anti-B220, and PNA staining (Fig. 2B). The GC surface and the proportion of B cell follicles containing GC peaked at 1 wk after OVA-Alum immunization in adult mice. Immunized neonates displayed a suboptimal GC response, characterized by a slower kinetics of induction and a reduced peak response (GC numbers and size) when compared with adults.

T_{FH} cell generation and localization in GC are impaired in neonates

We then sought to establish a correlation between the defective neonatal humoral response and the status of the T_{FH} cell response. As seen in Fig. 3A, OVA-Alum–immunized adult mice displayed an increased proportion of $CXCR5^+$ $PD\text{-}1^+$ cells in $CD4^+$ $CD19^-$ lymph node cells with an enhanced expression of the master regulator Bcl6 compared with unimmunized, Alum-treated mice. However, the percentages of these $CD4^+$ $CXCR5^+$ $PD\text{-}1^+$ T_{FH} cells in newborn lymph nodes were significantly reduced, and the Bcl6 expression was lower in comparison with adult T_{FH} cells. We next determined the localization of neonatal T_{FH} cells into lymphoid tissue by confocal microscopy. The T cell and B cell zones were visualized based, respectively, on CD3 and B220-specific staining, with GC B cells and T_{FH} cells specifically identified by the expression of the Bcl6 marker (Fig. 3B). The presence of T_{FH} cells in GC was determined at the peak of GC reaction for adult and neonatal mice, that is, 1 and 2 wk after immunization, respectively. Adult mice presented elevated numbers of $CD3^+$ $Bcl6^+$ T_{FH} cells in GC, in comparison with unimmunized mice. Although immunization of 1-wk-old mice induced increased numbers of T_{FH} cells, most of these cells were found in interfollicular regions (IFR) of lymph nodes, suggesting a defective migration pattern for neonatal T_{FH} cells toward GC. This was correlated with the incapacity of neonatal $CD4^+$ lymph node cells to properly downregulate the CCR7 chemokine receptor (Supplemental Fig. 3A) upon immunization. All of the $CXCR5^+$ $CD4^+$ lymph node cells were $CCR7^{low}$ in adults upon immunization, whereas a proportion of neonatal $CXCR5^+CD4^+$ lymph node cells remains $CCR7^{high}$. No particular increase of $PSGL\text{-}1^{low}$ $CD4^+$ cells, which have been reported to be localized in extrafollicular sites (23), could be detected in neonatal $CD4^+$ $CD19^-$ $CXCR5^+$ cells as compared with adults (Supplemental Fig. 3).

IL-4 deficiency limits the development of T_{FH} cells and prevents GC formation in immunized neonates

Because we observed a high secretion of IL-4 and IL-21, as well as double producers of these cytokines and a prominent production of IgE in neonates, we evaluated whether the T_{FH} cell function was linked to IL-4 in early life by immunizing IL-4–deficient newborns. As shown in Fig. 4A, proportions of $CXCR5^+$ $PD\text{-}1^+$ T_{FH} cells were comparable upon OVA-Alum immunization in adult $IL\text{-}4^{-/-}$ and wild-type (WT) mice. $IL\text{-}4^{-/-}$ neonates presented a slight

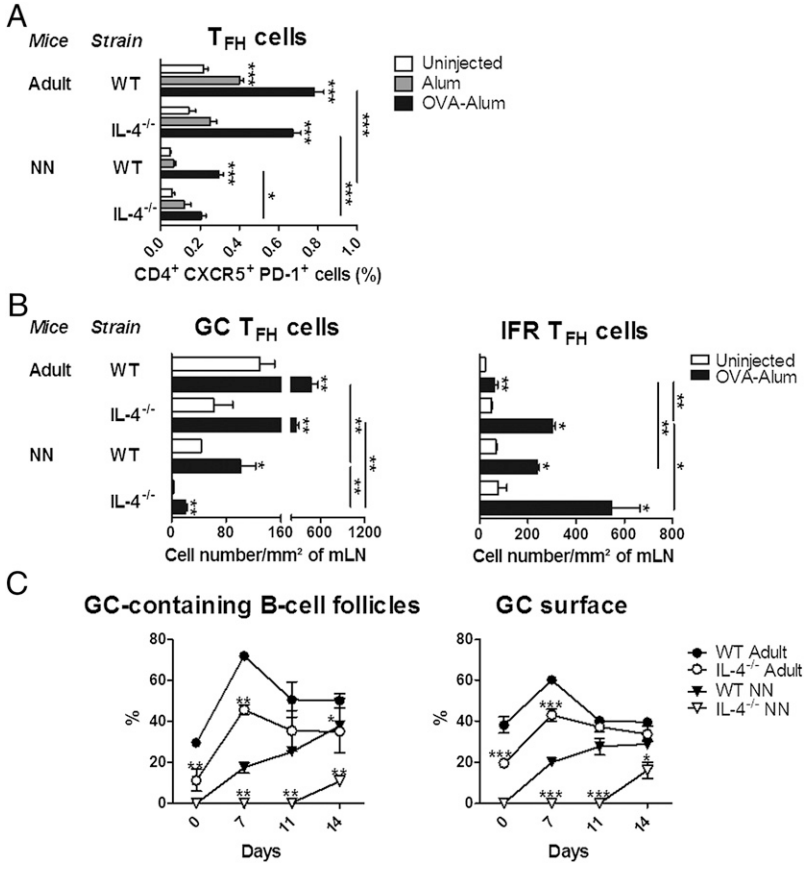

FIGURE 4. IL-4 promotes the development of T_{FH} cells and GC in newborns. Eight-wk-old and 7-d-old WT and $IL\text{-}4^{-/-}$ mice were immunized with OVA and Alum. (**A**) Proportion of $CD4^+$ $CD19^-$ $CXCR5^+$ $PD\text{-}1^+$ T_{FH} cells in mLN from WT or $IL\text{-}4^{-/-}$ 8-wk-old adult and 7-d-old neonatal mice on day 7 postimmunization. Groups contained two to seven mice. (**B**) Confocal analysis of the localization of T_{FH} cells in GC or IFR of mLN from WT ($n = 5$) or $IL\text{-}4^{-/-}$ adults ($n = 4$) on day 7 postimmunization, and from WT ($n = 5$) and $IL\text{-}4^{-/-}$ ($n = 4$) newborns on day 14 postimmunization. (**C**) The proportion of GC containing at least one GC and the surface of GC in B cell follicles were determined by histology. Groups contained four to five mice. Data were collected from two independent experiments. $^*p < 0.05$, $^{**}p < 0.005$, $^{***}p < 0.001$.

decreased percentage of T_{FH} cells in comparison with WT newborns. By assessing T_{FH} cell localization, we detected similar numbers of GC $CD3^+$ $Bcl6^+$ T_{FH} cells in adult WT and IL-$4^{-/-}$ mice, whereas IL-$4^{-/-}$ newborns displayed a strong decrease of GC T_{FH} cells compared with WT newborns (Fig. 4B). Correspondingly, we observed the strongest elevated numbers of T_{FH} cells in IFR of IL-$4^{-/-}$ neonates. These results suggest that IL-4 favors T_{FH} cell homing in GC in early life. We next wondered whether IL-4 could affect GC reaction in newborns. As shown in Fig. 4C, the proportion of B cell follicles containing GC was partially decreased in IL-$4^{-/-}$ adults compared with WT mice, whereas the GC surface was slightly reduced. In striking contrast, GC were barely detectable in IL-$4^{-/-}$ neonates and displayed smaller surface in comparison with WT newborns, indicating that IL-4 is particularly required for GC formation in early life.

Neonatal T_{FH} cells display Th17 characteristics in the absence of IL-4 that correlate with IgG2a production

To further characterize the impact of IL-4 on neonatal T_{FH} cells, we isolated $CD4^+$ $CD3^+$ $CXCR5^+$ $PD\text{-}1^+$ T_{FH} cells from OVA-Alum–immunized WT and IL-$4^{-/-}$ mice, and we analyzed their gene expression profile (Fig. 5A). In comparison with their respective $CD4^+$ $CD3^+$ $CXCR5^-$ $PD\text{-}1^-$ non-T_{FH} cells, adult and neonatal WT T_{FH} cells presented elevated amounts of Bcl6, IL-21, and IL-4 mRNA, with no significant impact on RORγt and IL-17 expression. Compared with adult T_{FH} cells, neonatal WT T_{FH} cells displayed reduced expression of Bcl6 and IL-4, as well as a lower induction of IL-21 mRNA, which confirmed the defective generation of T_{FH} lymphocytes in newborns. In comparison with WT T_{FH} cells, neonatal IL-$4^{-/-}$ T_{FH} cells presented reduced amounts of Bcl6 mRNA. Interestingly, we observed elevated levels of RORγt and IL-17 mRNA in neonatal IL-$4^{-/-}$ T_{FH} cells compared with WT newborns, suggesting that IL-4 regulates expression of Th17 features in neonatal T_{FH} cells. We confirmed this in vitro by showing that IL-6–polarized T cells from IL-$4^{-/-}$ neonates secreted reduced amounts of IL-21 compared with their WT counterparts, whereas IFN-γ production was not significantly affected (Fig. 5B). Strikingly, neonatal IL-$4^{-/-}$ T cells were the highest producers of IL-17 upon IL-6 stimulation.

Because we observed induction of a Th17-like phenotype in neonatal T_{FH} cells upon IL-4 deficiency, we next determined the Ab production in IL-$4^{-/-}$ neonates. We detected low amounts of total Ig in immunized IL-$4^{-/-}$ neonates compared with WT neonates, with a reduced secretion of IgG1 and a total inhibition of IgE (Fig. 6A). In contrast, we observed a significantly enhanced production of IgG2a in IL-$4^{-/-}$ newborns. Similarly, neonatal IL-$4^{-/-}$ T_{FH}-conditioned T cells strongly increased IgG2a class switching in vitro (Fig. 6B). These results suggest that IL-4–mediated responses in early life hamper an IL-17–dependent IgG2a production.

Discussion

In this study, we showed that emergence of T_{FH} cells upon immunization in neonates is impaired and that IL-4 favors the generation of these lymphocytes in early life. Indeed, we detected lower proportion and limited localization in GC of T_{FH} cells in neonatal lymphoid tissues. These effects were greatly enhanced in the case of IL-4 deficiency. In addition, immunized newborns presented decreased Ab production and maturation, as well as reduced and delayed GC reaction, suggesting that the impaired T_{FH} cell response of neonates was associated with their defective humoral response.

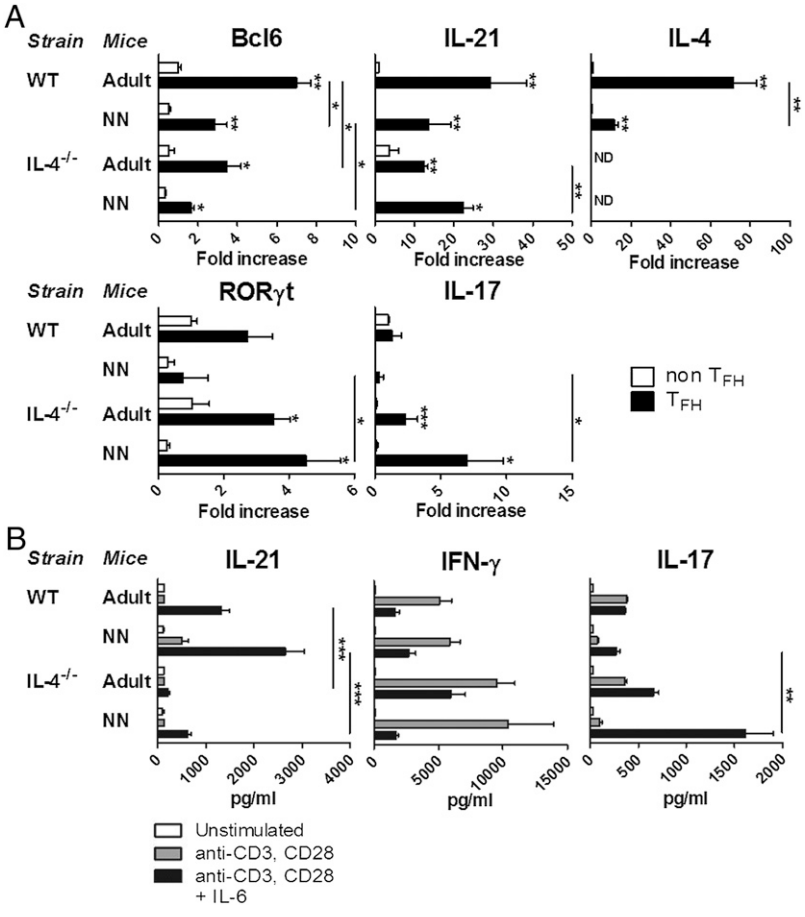

FIGURE 5. IL-4 regulates the Th17 profile of neonatal T_{FH} cells. (**A**) Gene expression analysis of $CD4^+$ $CD3^+$ $CXCR5^+$ $PD\text{-}1^+$ T_{FH} cells and $CD4^+$ $CD3^+$ $CXCR5^-$ $PD\text{-}1^-$ non-T_{FH} cells isolated from mLN of 8-wk-old and 7-d-old WT and IL-$4^{-/-}$ immunized mice 7 d after immunization. Each FACS sorting was performed with at least five adult and eight newborn mice. Cytokine levels were normalized using β-actin mRNA as a reference and relatively expressed against values obtained with non-T_{FH} cells from adult WT mice and were collected from at least two independent experiments. (**B**) $CD4^+$ T cells isolated from spleens of 8-wk-old and 7-d-old WT or IL-$4^{-/-}$ mice were stimulated with anti-CD3 and anti-CD28 mAb in the presence or absence of IL-6. Cytokine levels in supernatants were measured by ELISA. Data were collected from at least three independent experiments each performed with groups of 4 adult and 20 neonatal mice. $*p < 0.05$, $**p < 0.005$, $***p < 0.001$.

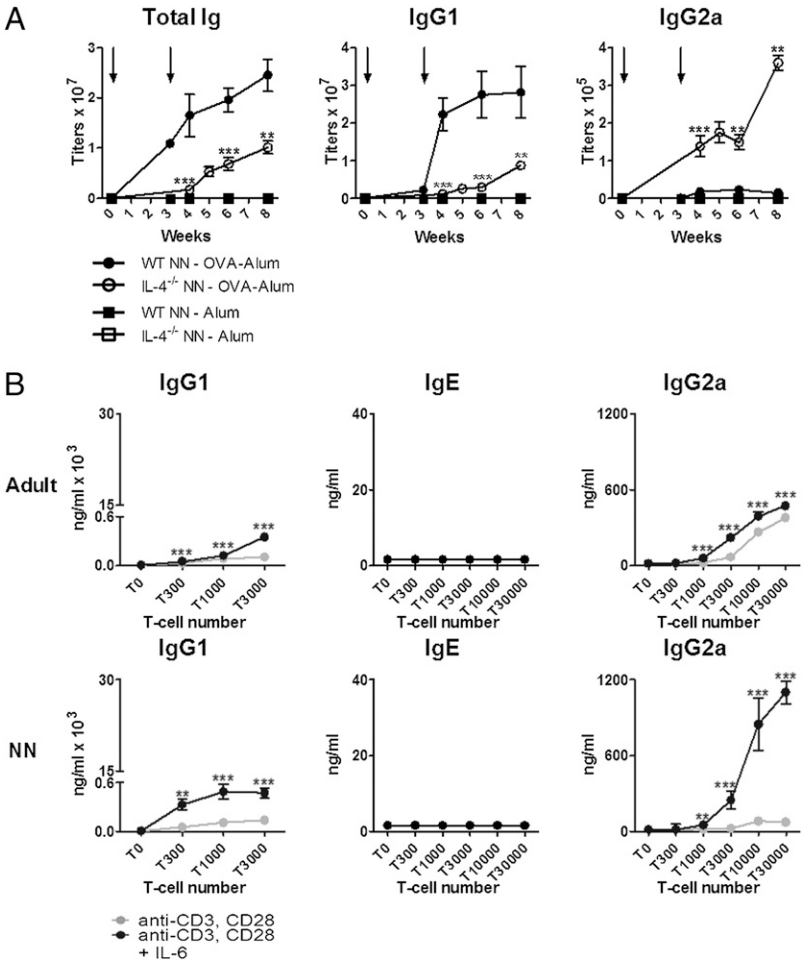

FIGURE 6. IL-4 deficiency favors IgG2a production in newborns. (**A**) Eight-week-old (n = 5) and 7-d-old (n = 6) IL-$4^{-/-}$ mice were immunized with OVA and Alum. OVA-specific serum Ig levels were measured by ELISA. (**B**) $CD4^+$ T cells isolated from spleens of 8-wk-old and 7-d-old IL-$4^{-/-}$ mice were stimulated with anti-CD3 and anti-CD28 mAb and were cocultured with B cells isolated from spleens of 8-wk-old adult WT mice, in the presence of anti-CD3 mAb. Ig levels in supernatants were quantified by ELISA. Data are mean values ± SEM from five independent experiments each performed with quadruplicate cultures of pooled groups of 4 adult and 20 neonatal mice. $^{**}p < 0.005$, $^{***}p < 0.001$.

Although the pathway of T_{FH} cell differentiation is a matter of debate, IL-6 is considered as one of its inducers (20, 21). This cytokine indeed promoted production of IL-21 and enhanced the B cell help capacity of neonatal T cells, suggesting that these lymphocytes have no intrinsic defect to differentiate into T_{FH} cells. Moreover, IL-6 increased expression of ICOS on neonatal T cells. Several studies reported an important role for ICOS in T_{FH} cell differentiation. This costimulatory molecule regulates secretion of IL-21, another inducer of the T_{FH} cell pathway, in T_{FH} cells, and induces the expression of the master regulator Bcl6 (19, 24). ICOS is also involved in interactions between T_{FH} cells and B cells, the latter being required for T_{FH} cell generation (21). Cell contact between T_{FH} cells and B lymphocytes could be hampered in early life. We indeed previously demonstrated that CD40L expression is defective on neonatal T cells (25) and in this study observed a limited expression of ICOS on stimulated neonatal $CD4^+$ T cells compared with adult ones. This limited expression of ICOS could account for the lower expression of Bcl6 that we observed on neonatal $CD4^+$ T cells both in vitro and in vivo. On the B cell side, costimulatory molecules are poorly expressed by neonatal B cells (3). Impaired interactions between those cell types could account for the low proportions of T_{FH} cells we detected in neonates, for their lower expression of the master regulator Bcl6, as well as for their confinement in IFR where the initiation of T_{FH} cell development occurs (26). The weak presence of neonatal T_{FH} cells in GC is linked to an inefficient downregulation of the chemokine receptor CCR7, but could also be due to an insufficient production of the chemokine CXCL13 by FDC, because these cells present a delayed maturation in early life (5). Furthermore, a model of T_{FH} cell differentiation suggests that full differentiation of T_{FH} cells occurs in GC, where T_{FH} cells express their highest levels of Bcl6 (14). The particular localization of neonatal T_{FH} cells may therefore explain the limited T_{FH} cell differentiation in early life.

This work highlights a particular contribution of IL-4 in the emergence of neonatal T_{FH} cells. IL-4–deficient newborns indeed displayed decreased numbers of T_{FH} cells that were mainly localized outside of GC. IL-4 could indirectly promote the generation of T_{FH} cells in early life by stimulating neonatal B lymphocytes (12). Strong inhibition of GC reaction and of Ab production in immunized IL-$4^{-/-}$ newborns supports this idea. In addition, compared with their WT counterparts and with the IL-$4^{-/-}$ adult $CD4^+$ T cells, neonatal IL-$4^{-/-}$ $CD4^+$ T cells did not sustain B cell proliferation in vitro (data not shown). IL-4 might also somehow impact on other negative signals potentially generated by neonatal B cells. Indeed, an eventual higher frequency of IL-10–producing or programmed cell death ligand 1–expressing B cells, both parameters that may affect T_{FH} cell function, as recently described during HIV infection (27), may be present in neonatal GC. Further investigations would clarify how IL-4 may affect these B cell phenotypes.

Alternatively, neonatal T_{FH} cells could share Th2 features, as already described in helminth infection (28) and as shown in this study. We indeed observed coproduction of IL-21 and IL-4 by neonatal T_{FH}-conditioned T cells, as well as a significant Bcl6, IL-21, and IL-4 mRNA induction in isolated neonatal $CD4^+$ $CD3^+$ $CXCR5^+$ $PD\text{-}1^+$ T_{FH} cells compared with non-T_{FH} cells. Furthermore, recent works indicated that the enhancer CNS-2 in the *Il4* locus was essential for IL-4 production by adult T_{FH} cells,

a mechanism distinct from the one of Th2 cells (29, 30). The regulatory function of this genetic region could be impaired in early life, as supported by the lower expression of IL-4 mRNA we detected in neonatal WT $CD4^+$ $CD3^+$ $CXCR5^+$ $PD\text{-}1^+$ T_{FH} cells compared with adult T_{FH} cells. Additionally, another regulatory region of the *Il4* locus, CNS-1, was shown to be hypomethylated in neonatal $CD4^+$ T cells, allowing a rapid and high production of IL-4 (8). Whether CNS-1 could also affect IL-4 secretion by neonatal T_{FH} cells remains to be established.

The Th2-like phenotype of neonatal T_{FH} cells may account for the induction of IgE production in newborns. We indeed observed that the IgE response of newborns was less affected compared with their other isotype responses. However, neonatal IgE exhibited low Ag affinity. This reduced affinity maturation could be related to the limited T_{FH} cell generation and localization in GC in neonates, as well as to their weak secretion of IgG1. Indeed, production of high-affinity IgE is hampered in IgG1-deficient mice (31). On the B cell side of view, default in the selection of neonatal high-affinity B cells and the stronger tendency for immature B cells to produce IgE (32, 33) could account for the low Ag affinity presented by neonatal IgE.

In contrast, IL-4 appears to directly affect the genetic profile of neonatal T_{FH} cells. T_{FH} cells of IL-4–deficient newborns increased their expression of RORγt and IL-17, both hallmarks of Th17 cells, without acquiring a Th1 profile. This is in agreement with the reported capacity of T_{FH} cells to produce IL-17 (24), a cytokine that is involved in the modulation of humoral immunity (34, 35) and in IgG2a production (36). Accordingly, we detected an enhanced secretion of IgG2a in immunized IL-4–deficient neonates and in cocultures with neonatal $IL\text{-}4^{-/-}$ T_{FH}-conditioned T cells. This suggests that IL-4 dampens IL-17–dependent IgG2a B cell isotype class switching in early life and favors IgE production.

Limited infant B cell response to vaccines that are reported in humans and are associated with a poor titer of persistent protective Abs and defective GC induction (3) may be due in part to the diminished neonatal T_{FH} cell differentiation and trafficking described in this study. Furthermore, the infant limited protective Th1-type response that was to date associated with a predominance of Th17-type response combined with multiple cellular sources of IL-10, including B cells, could be revisited with the potential development of Th2-like T_{FH} cells that control these Th17 cells, especially in the case of infant Th2-biased responses to hepatitis B virus and oral poliovirus vaccines (2).

In conclusion, our work demonstrates that T_{FH} cell responses can be induced in newborns, but that their full development is impaired, as reported in a recent study (37). Indeed, an adult-like ratio of $CD4^+$ $CXCR5^+$ $PD\text{-}1^+$ cells/$CD4^+$ $CXCR5^-$ $PD\text{-}1^-$ cells was not reached in C57BL/6 neonates immunized with tetanus toxoid. We further showed in this study that, in contrast to adult, neonatal $CD3^+$ $Bcl6^+$ T_{FH} cells are confined in interfollicular regions rather than in GC after immunization. Additionally, we propose that IL-4 represents an important regulator of the generation and the plasticity of T_{FH} cells in early life, as well as a critical component of neonatal humoral immunity. Our observations could be of interest in the field of neonatal and pediatric vaccines. Development of new adjuvants enhancing T_{FH} cell responses in early life may indeed promote protective humoral immunity and therefore limit the need of several vaccine recalls in newborns.

Acknowledgments

We thank Fabienne Andris and Fouad Eddhari for helpful discussion and technical advice; Luis Graca for technical advice; Frédéric Paulart for technical assistance; and Philippe Horlait, Laurent Depret, Christophe Notte, Grégory Waterlot, and Samuel Vander Bist for animal care.

Disclosures

The authors have no financial conflicts of interest.

References

1. Siegrist, C. A. 2001. Neonatal and early life vaccinology. *Vaccine* 19: 3331–3346.
2. Adkins, B., C. Leclerc, and S. Marshall-Clarke. 2004. Neonatal adaptive immunity comes of age. *Nat. Rev. Immunol.* 4: 553–564.
3. Siegrist, C. A., and R. Aspinall. 2009. B-cell responses to vaccination at the extremes of age. *Nat. Rev. Immunol.* 9: 185–194.
4. Fu, Y. X., and D. D. Chaplin. 1999. Development and maturation of secondary lymphoid tissues. *Annu. Rev. Immunol.* 17: 399–433.
5. Pihlgren, M., C. Tougne, P. Bozzotti, A. Fulurija, M. A. Duchosal, P. H. Lambert, and C. A. Siegrist. 2003. Unresponsiveness to lymphoid-mediated signals at the neonatal follicular dendritic cell precursor level contributes to delayed germinal center induction and limitations of neonatal antibody responses to T-dependent antigens. *J. Immunol.* 170: 2824–2832.
6. Pihlgren, M., N. Schallert, C. Tougne, P. Bozzotti, J. Kovarik, A. Fulurija, M. Kosco-Vilbois, P. H. Lambert, and C. A. Siegrist. 2001. Delayed and deficient establishment of the long-term bone marrow plasma cell pool during early life. *Eur. J. Immunol.* 31: 939–946.
7. Zaghouani, H., C. M. Hoeman, and B. Adkins. 2009. Neonatal immunity: faulty T-helpers and the shortcomings of dendritic cells. *Trends Immunol.* 30: 585–591.
8. Rose, S., M. Lichtenheld, M. R. Foote, and B. Adkins. 2007. Murine neonatal CD4+ cells are poised for rapid Th2 effector-like function. *J. Immunol.* 178: 2667–2678.
9. Li, L., H. H. Lee, J. J. Bell, R. K. Gregg, J. S. Ellis, A. Gessner, and H. Zaghouani. 2004. IL-4 utilizes an alternative receptor to drive apoptosis of Th1 cells and skews neonatal immunity toward Th2. *Immunity* 20: 429–440.
10. Debock, I., S. Delbauve, A. Dubois, M. Pétein, O. Leo, M. Goldman, and V. Flamand. 2012. Th17 alloimmunity prevents neonatal establishment of lymphoid chimerism in IL-4-deprived mice. *Am. J. Transplant.* 12: 81–89.
11. Berton, M. T., J. W. Uhr, and E. S. Vitetta. 1989. Synthesis of germ-line gamma 1 immunoglobulin heavy-chain transcripts in resting B cells: induction by interleukin 4 and inhibition by interferon gamma. *Proc. Natl. Acad. Sci. USA* 86: 2829–2833.
12. Paul, W. E., and J. Ohara. 1987. B-cell stimulatory factor-1/interleukin 4. *Annu. Rev. Immunol.* 5: 429–459.
13. Rothman, P., S. Lutzker, W. Cook, R. Coffman, and F. W. Alt. 1988. Mitogen plus interleukin 4 induction of C epsilon transcripts in B lymphoid cells. *J. Exp. Med.* 168: 2385–2389.
14. Crotty, S. 2011. Follicular helper CD4 T cells (TFH). *Annu. Rev. Immunol.* 29: 621–663.
15. Johnston, R. J., A. C. Poholek, D. DiToro, I. Yusuf, D. Eto, B. Barnett, A. L. Dent, J. Craft, and S. Crotty. 2009. Bcl6 and Blimp-1 are reciprocal and antagonistic regulators of T follicular helper cell differentiation. *Science* 325: 1006–1010.
16. Nurieva, R. I., Y. Chung, G. J. Martinez, X. O. Yang, S. Tanaka, T. D. Matskevitch, Y. H. Wang, and C. Dong. 2009. Bcl6 mediates the development of T follicular helper cells. *Science* 325: 1001–1005.
17. Yu, D., S. Rao, L. M. Tsai, S. K. Lee, Y. He, E. L. Sutcliffe, M. Srivastava, M. Linterman, L. Zheng, N. Simpson, et al. 2009. The transcriptional repressor Bcl-6 directs T follicular helper cell lineage commitment. *Immunity* 31: 457–468.
18. Deenick, E. K., A. Chan, C. S. Ma, D. Gatto, P. L. Schwartzberg, R. Brink, and S. G. Tangye. 2010. Follicular helper T cell differentiation requires continuous antigen presentation that is independent of unique B cell signaling. *Immunity* 33: 241–253.
19. Choi, Y. S., R. Kageyama, D. Eto, T. C. Escobar, R. J. Johnston, L. Monticelli, C. Lao, and S. Crotty. 2011. ICOS receptor instructs T follicular helper cell versus effector cell differentiation via induction of the transcriptional repressor Bcl6. *Immunity* 34: 932–946.
20. Eddahri, F., S. Denanglaire, F. Bureau, R. Spolski, W. J. Leonard, O. Leo, and F. Andris. 2009. Interleukin-6/STAT3 signaling regulates the ability of naive T cells to acquire B-cell help capacities. *Blood* 113: 2426–2433.
21. Nurieva, R. I., Y. Chung, D. Hwang, X. O. Yang, H. S. Kang, L. Ma, Y. H. Wang, S. S. Watowich, A. M. Jetten, Q. Tian, and C. Dong. 2008. Generation of T follicular helper cells is mediated by interleukin-21 but independent of T helper 1, 2, or 17 cell lineages. *Immunity* 29: 138–149.
22. Vogelzang, A., H. M. McGuire, D. Yu, J. Sprent, C. R. Mackay, and C. King. 2008. A fundamental role for interleukin-21 in the generation of T follicular helper cells. *Immunity* 29: 127–137.
23. Odegard, J. M., B. R. Marks, L. D. DiPlacido, A. C. Poholek, D. H. Kono, C. Dong, R. A. Flavell, and J. Craft. 2008. ICOS-dependent extrafollicular helper T cells elicit IgG production via IL-21 in systemic autoimmunity. *J. Exp. Med.* 205: 2873–2886.
24. Bauquet, A. T., H. Jin, A. M. Paterson, M. Mitsdoerffer, I. C. Ho, A. H. Sharpe, and V. K. Kuchroo. 2009. The costimulatory molecule ICOS regulates the expression of c-Maf and IL-21 in the development of follicular T helper cells and TH-17 cells. *Nat. Immunol.* 10: 167–175.
25. Flamand, V., V. Donckier, F. X. Demoor, A. Le Moine, P. Matthys, M. L. Vanderhaeghen, Y. Tagawa, Y. Iwakura, A. Billiau, D. Abramowicz, and M. Goldman. 1998. CD40 ligation prevents neonatal induction of transplantation tolerance. *J. Immunol.* 160: 4666–4669.
26. Kerfoot, S. M., G. Yaari, J. R. Patel, K. L. Johnson, D. G. Gonzalez, S. H. Kleinstein, and A. M. Haberman. 2011. Germinal center B cell and T follicular helper cell development initiates in the interfollicular zone. *Immunity* 34: 947–960.

27. Cubas, R. A., J. C. Mudd, A. L. Savoye, M. Perreau, J. van Grevenynghe, T. Metcalf, E. Connick, A. Meditz, G. J. Freeman, G. Abesada-Terk, Jr., et al. 2013. Inadequate T follicular cell help impairs B cell immunity during HIV infection. *Nat. Med.* 19: 494–499.
28. Glatman Zaretsky, A., J. J. Taylor, I. L. King, F. A. Marshall, M. Mohrs, and E. J. Pearce. 2009. T follicular helper cells differentiate from Th2 cells in response to helminth antigens. *J. Exp. Med.* 206: 991–999.
29. Harada, Y., S. Tanaka, Y. Motomura, Y. Harada, S. Ohno, S. Ohno, Y. Yanagi, H. Inoue, and M. Kubo. 2012. The 3′ enhancer CNS2 is a critical regulator of interleukin-4-mediated humoral immunity in follicular helper T cells. *Immunity* 36: 188–200.
30. Vijayanand, P., G. Seumois, L. J. Simpson, S. Abdul-Wajid, D. Baumjohann, M. Panduro, X. Huang, J. Interlandi, I. M. Djuretic, D. R. Brown, et al. 2012. Interleukin-4 production by follicular helper T cells requires the conserved Il4 enhancer hypersensitivity site V. *Immunity* 36: 175–187.
31. Xiong, H., J. Dolpady, M. Wabl, M. A. Curotto de Lafaille, and J. J. Lafaille. 2012. Sequential class switching is required for the generation of high affinity IgE antibodies. *J. Exp. Med.* 209: 353–364.
32. Erazo, A., N. Kutchukhidze, M. Leung, A. P. Christ, J. F. Urban, Jr., M. A. Curotto de Lafaille, and J. J. Lafaille. 2007. Unique maturation program of the IgE response in vivo. *Immunity* 26: 191–203.
33. Wesemann, D. R., J. M. Magee, C. Boboila, D. P. Calado, M. P. Gallagher, A. J. Portuguese, J. P. Manis, X. Zhou, M. Recher, K. Rajewsky, et al. 2011. Immature B cells preferentially switch to IgE with increased direct Sμ to Sε recombination. *J. Exp. Med.* 208: 2733–2746.
34. Hsu, H. C., P. Yang, J. Wang, Q. Wu, R. Myers, J. Chen, J. Yi, T. Guentert, A. Tousson, A. L. Stanus, et al. 2008. Interleukin 17-producing T helper cells and interleukin 17 orchestrate autoreactive germinal center development in autoimmune BXD2 mice. *Nat. Immunol.* 9: 166–175.
35. Peters, A., L. A. Pitcher, J. M. Sullivan, M. Mitsdoerffer, S. E. Acton, B. Franz, K. Wucherpfennig, S. Turley, M. C. Carroll, R. A. Sobel, et al. 2011. Th17 cells induce ectopic lymphoid follicles in central nervous system tissue inflammation. *Immunity* 35: 986–996.
36. Nakae, S., A. Nambu, K. Sudo, and Y. Iwakura. 2003. Suppression of immune induction of collagen-induced arthritis in IL-17-deficient mice. *J. Immunol.* 171: 6173–6177.
37. Mastelic, B., A. T. Kamath, P. Fontannaz, C. Tougne, A. F. Rochat, E. Belnoue, C. Combescure, F. Auderset, P. H. Lambert, F. Tacchini-Cottier, and C. A. Siegrist. 2012. Environmental and T cell-intrinsic factors limit the expansion of neonatal follicular T helper cells but may be circumvented by specific adjuvants. *J. Immunol.* 189: 5764–5772.